[Supplementary material]

The origins of decorated ostrich eggs in the ancient Mediterranean and Middle East

Tamar Hodos[1,*], Caroline R. Cartwright[2], Janet Montgomery[3], Geoff Nowell[4], Kayla Crowder[3], Alexandra C. Fletcher[5] & Yvonne Gönster[6]

[1] *Department of Anthropology and Archaeology, University of Bristol, UK*

[2] *Department of Scientific Research, The British Museum, London, UK*

[3] *Department of Archaeology, Durham University, UK*

[4] *Department of Earth Sciences, Durham University, UK*

[5] *Department of the Middle East, The British Museum, London, UK*

[6] *Deutsches Schloss- und Beschlägemuseum, Velbert, Germany*

[*] *Author for correspondence (Email: t.hodos@bristol.ac.uk)*

Materials and methods

Scanning Electron Microscopy (SEM)

For SEM, the VP mode enabled the observation of non-conductive specimens without the need for coating, vital for most museum objects. All specimens were examined with 40P chamber pressure, which was used to eliminate surface charging on non-conducting ostrich eggshell. Each specimen was placed on an aluminium SEM stub for examination, mostly with an accelerating voltage of 15kV using the backscatter electron detector. For the modern ostrich egg shell (OES), this was often lowered to 10kV, on account of the fresh condition of the specimens. For optimal visualisation of detail, the working distance varied from 38.5mm to 12mm. The magnification ranged from ×12 to ×500 as dictated by the individual fragment being examined. This aspect of the study was undertaken in the British Museum's Department of Scientific Research.

Isotope analysis

All tools and surfaces were cleaned between each sample with a 2% Decon solution to minimize sample contamination. The modern OES were cleaned of debris by removing the crystalline outer layer and membranous inner layer. This was achieved using a diamond dental burr and a hand-held drill. Multiple samples were taken from each modern OES to test the isotopic homogeneity and the strontium concentrations across the shell in order to determine how much OES needed to be removed from archaeological eggs for analysis. Approximately 1–3mg of modern OES was then placed in a sealed container and transferred to the laboratory facilities at the University of Durham's Department of Earth Sciences for strontium compositional analysis and an additional duplicate set of samples to the NERC Isotope Geosciences Laboratories in Keyworth for oxygen and carbon isotope analysis.

The archaeological OES samples available for analysis were small and ranged from 12 to 44mg prior to cleaning. All surfaces and debris were removed with a diamond dental burr and a hand-held drill and discarded. Two archaeological OES samples from Naukratis (985) and Ur (982), for which larger than average samples were provided, were then subject to a gentle leaching protocol to attempt to remove any diagenetic strontium prior to preparing the main batch. Samples were leached for 30 minutes at room temperature in MQ H_2O, monitored throughout to ensure the sample did not disintegrate, and the leachate reserved. This was repeated and the leachate again reserved. The strontium isotope ratio of both leaches and the OES sample were then measured. Negligible differences were found (i.e. <0.00016) between the isotope ratio of sequential leachates and the leached OES at both sites, indicating the leached strontium had very similar isotope ratios to that of the OES. Following this, the archaeological OES samples were subjected to one leach of 30 minutes at room temperature prior to strontium isotope analysis.

Strontium isotope ($^{87}Sr/^{86}Sr$) and concentration (Sr ppm) analysis was conducted at the Durham Geochemistry Centre in the Earth Science Department of Durham University (UK). The OES samples were prepared using the column chemistry methods outlined in Charlier *et al.* (2006). Samples were placed on a hot plate (100°C) overnight to dissolve in 500µl of nitric acid (HNO_3). Each column was loaded with 80µl of Eichrom Sr specific resin which was then cleaned and preconditioned. Two rounds of 250µl 3 N HNO_3 was rinsed through the column to elute waste. Next, two rounds of 200µl MilliQ water (MQ H_2O) was passed through the columns to elute the strontium fraction. Once collected, each sample was acidified to yield a solution of 3% HNO_3 for analysis. The ^{86}Sr beam was measured to determine the strontium concentrations for each sample. The beam intensity determined the dilution factor for each sample so that each would yield a beam size of approximately 20 V ^{88}Sr to match the International Isotopic Reference Material (IRM), NBS987. The strontium samples were analysed using a Neptune Multi-Collector Inductively Coupled Plasma Mass Spectrometry (MC-ICP-MS). An ESI PFA-50 nebulizer and a micro-cyclonic spray chamber were used to introduce the sample. Instrumental mass bias was corrected by using $^{88}Sr/^{86}Sr$ ratio of 8.375209 (reciprocal of $^{86}Sr/^{88}Sr$ ratio of 0.1194) and an exponential law. Isobaric interferences from Kr and Rb on ^{87}Sr and ^{86}Sr were corrected using ^{83}Kr and ^{85}Rb as monitor masses. International reference standard NBS987 was used to do determine reproducibility.

The mean $^{87}Sr/^{86}Sr$ ratio and reproducibility for IRM NBS987 was 0.71026 ± 0.000012 (2σ, n = 26).

Oxygen ($\delta^{18}O$) and carbon ($\delta^{13}C$) isotope analyses were conducted at the NERC Isotope Geoscience Facilities at the British Geological Survey (UK). The modern samples were split into two and one set plasma ashed to remove organics and determine if the resulting values differed. The methodology followed was that outlined in Chenery *et al.* (2012: 310). Approximately 1–3mg of clean eggshell sample was placed in glass vials with sealed septa and placed on a Multiprep system (GV Instruments) hot block (90°C). The vials were evacuated, and four drops of anhydrous phosphoric acid were added. The CO_2 resultant was cryogenically collected for 14 minutes. Oxygen ($\delta^{18}O$) and carbon ($\delta^{13}C$) values were measured using a GV IsoPrime dual inlet mass spectrometer and the results reported in parts per thousand (‰). All results were normalised to Vienna Pee Dee Belemnite (VPDB) and an in-house carbonate standard, Keyworth Carrera Marble, and calibrated against certified reference material (NBS19). Carbonate (VPDB) values were converted using the equation of Coplen (1988): ($\delta^{18}O_{VSMOW} = 1.03091 \times \delta^{18}O_{VPDB} + 30.91$). Analytical uncertainty was estimated at ±0.02 ‰ (1σ, n = 24) for $\delta^{13}C$ and for $\delta^{18}O$ ±0.04 ‰ (1σ, n = 24).

Results and discussion

Data are tabulated in Tables S1 and S2. Multiple samples were taken from each modern OES to test homogeneity and excellent repeatability was found across each egg (Table S1). The $^{87}Sr/^{86}Sr$ isotope ratios range from 0.70742 to 0.70930 (mean: 0.70833, 1σ = 0.00039, n = 44). Strontium concentrations range from 62 to 1251 ppm (mean: 403, 1σ = 230, n = 42). The $\delta^{18}O_{VPDB}$ values range from -6.5 to 17.6‰ (mean: 3.0, 1σ = 5.0, n = 44) and $\delta^{13}C_{VPDB}$ samples from -10.9 to 2.5‰ (mean: -7.0, 1σ = 3.7, n = 44). Modern carbon isotope data ($\delta^{13}C$) have not been adjusted to account for the Suess Effect and may be ~1.5‰ lower than equivalent archaeological data (Suess 1958; Friedli *et al.* 1986; Marino & McElroy 1991). The modern samples were plasma ashed to remove any organics and this shifted the data marginally more than the experimental error ($\delta^{13}C$, -0.5‰) (Table S1).

Table S1. Oxygen, carbon and strontium isotopes and concentration for modern ostrich egg shell. Data are mean values of different samples taken to assess intra-egg homogeneity. Values for plant* $\delta^{13}C$ are calculated using the OES diet-carbonate offset of -16.2‰ reported by von Schirnding *et al*. (1982). Values for drinking water are calculated using the equation of Johnson *et al*. (1998): $\delta^{18}O_{dw}$ = 31.8 + 0.65 × $\delta^{18}O_{carb}$. Analytical reproducibility was estimated at: ± 0.02‰ (1sd) for $\delta^{13}C$; ± 0.04‰ (1sd) for $\delta^{18}O$; ± 0.000012 (2sd) for $^{87}Sr/^{86}Sr$.**

Country	Site	Lab code	n	Treatment	$\delta^{13}C_{PDB}$ ‰		$\delta^{13}C_{PDB}$ ‰	$\delta^{18}O_{PDB}$ ‰		$\delta^{18}O_{VSMOW}$ ‰		$\delta^{18}O_{VSMOW}$ ‰	Lab code	n	$^{87}Sr/^{86}Sr$ norm	2SE	Sr ppm
					mean	sd	plant*	mean	sd	mean	sd	drinking water**					
		784 (a-e)	5	Plasma ashed	-3.27	0.12	-19.47	1.67	0.05	32.58	0.05	1.2					
Egypt	Alexandria	784 (a-e)	5	Unashed	-3.16	0.12	-19.36	1.92	0.07	32.84	0.07	1.6	783 (a,b,c)	3	0.708455	0.000006	173
Israel	Gal'ed	2094 (a-c)	3	Unashed	-3.12	0.27	-19.32	-5.07	0.04	25.69	0.04	-9.4	2094a	1	0.707621	0.000013	124
	Azraq	2095a (1-3)	3	Unashed	-4.86	0.02	-21.06	0.21	0.03	31.14	0.03	-1.0	2095a	1	0.708270	0.000008	423
Jordan	Wetlands Reserve	2095b (1-3)	3	Unashed	-9.22	0.04	-25.42	-3.80	0.11	27.00	0.09	-7.4	2095b	1	0.707906	0.000012	69
		782 (a-e)	5	Plasma ashed	-7.04	0.02	-23.24	-6.53	0.05	24.13	0.06	-11.8					
Turkey	Çanakkale	782 (a-e)	5	Unashed	-6.87	0.04	-23.07	-6.24	0.10	24.43	0.11	-11.3	781 (a,b,c)	3	0.708061	0.000005	70

Table S2. Oxygen, carbon and strontium isotopes and concentration for archaeological ostrich egg shell. Samples 982 and 985 are the two samples subjected to leaching to assess diagenetic strontium and the shell data is the value after leaching. Modern OES samples have not been corrected for the Suess (1958) offset. Values for plant* $\delta^{13}C$ are calculated using the OES diet-carbonate offset of -16.2‰ reported by von Schirnding *et al*. (1982). Values for drinking water are calculated using the equation of Johnson *et al*. 1998: $\delta^{18}O_{dw}$ = 31.8 + 0.65 × $\delta^{18}O_{carb}$. Analytical reproducibility was estimated at: ± 0.02‰ (1sd) for $\delta^{13}C$; ± 0.04‰ (1sd) for $\delta^{18}O$; ± 0.000012 (2sd) for $^{87}Sr/^{86}Sr$.**

Country	Site	Lab code	British Museum registration numbers	$\delta^{13}C_{PDB}$ ‰	$\delta^{13}C_{PDB}$ ‰	$\delta^{18}O_{PDB}$ ‰	$\delta^{18}O_{VSMOW}$ ‰	$\delta^{18}O_{VSMOW}$ ‰	$^{87}Sr/^{86}Sr$ norm	2SE	Sr ppm
				OES	plant*	OES	OES	drinking water**			
Bahrain	A'Ali	968	1889.1213.11 (136243) (a)	-9.4	-25.6	5.2	36.3	6.9	0.708272	0.000013	468
Bahrain	A'Ali	972	1889.1213.11 (136243 (b)	-1.4	-17.6	8.7	39.9	12.5	0.708244	0.000009	914
Cyprus	Salamis	965	1967.1104.12	-9.2	-25.4	1.4	32.3	0.8	0.708970	0.000011	214
Egypt	Mostagedda	977	Pan grave bead 1930.0711.291 ea63268	-10.3	-26.5	2.9	34.0	3.3	0.707797	0.000011	231

Country	Site	Lab code	British Museum registration numbers	$\delta^{13}C_{PDB}$ ‰	$\delta^{13}C_{PDB}$ ‰	$\delta^{18}O_{PDB}$ ‰	$\delta^{18}O_{VSMOW}$ ‰	$\delta^{18}O_{VSMOW}$ ‰	$^{87}Sr/^{86}Sr$ norm	2SE	Sr ppm
				OES	plant*	OES	OES	drinking water**			
Egypt	Naukratis, Temple of Apollo	979	1888.0601.85 (1)	-10.6	-26.8	2.5	33.5	2.7	0.708521	0.000011	433
Egypt	Naukratis, Temple of Apollo	981	1888.0601.85 (2)	-6.9	-23.1	4.5	35.6	5.9	0.708136	0.000010	778
Egypt	Naukratis, Temple of Apollo	980	1888.0601.85 (3)	-9.4	-25.6	-0.4	30.6	-1.9	0.708581	0.000013	299
Egypt	Naukratis, Temple of Apollo	995	1888.0601.85 (4)	-8.5	-24.7	1.5	32.5	1.0	0.708582	0.000010	275
Egypt	Naukratis, Temple of Apollo	987	1888.0601.85 (5)	-10.6	-26.8	2.2	33.2	2.2	0.708566	0.000009	504
Egypt	Naukratis, Temple of Apollo	993	1888.0601.85 (6)	-3.2	-19.4	1.0	31.9	0.2	0.708743	0.000012	434

Country	Site	Lab code	British Museum registration numbers	$\delta^{13}C_{PDB}$ ‰	$\delta^{13}C_{PDB}$ ‰	$\delta^{18}O_{PDB}$ ‰	$\delta^{18}O_{VSMOW}$ ‰	$\delta^{18}O_{VSMOW}$ ‰	$^{87}Sr/^{86}Sr$ norm	2SE	Sr ppm
				OES	**plant***	**OES**	**OES**	**drinking water****			
Egypt	Naukratis, Temple of Apollo	991	1888.0601.85 (7)	-9.7	-25.9	5.4	36.5	7.3	0.708414	0.000009	533
Egypt	Naukratis, Temple of Apollo	989	1888.0601.85 (8)	-9.1	-25.3	5.0	36.1	6.6	0.708419	0.000008	506
Egypt	Naukratis, Temple of Apollo	986	1888.0601.85 (9)	-6.9	-23.1	4.6	35.7	5.9	0.708145	0.000008	643
Egypt	Naukratis, Temple of Apollo	985	1888.0601.85a G&R	-10.8	-27.0	1.4	32.4	0.9	0.708530	0.000005	**n.d.**
		985	leachate 1						0.708461	0.000007	
		985	leachate 2						0.708373	0.000007	
Egypt	Naukratis, Temple of Apollo	2092	18,860,401.16	-9.5	-25.7	7.3	38.5	10.2	0.708183	0.000008	516
Egypt	Bir Kiseiba	2093	20,040,517.36	1.6	-14.6	8.7	39.8	12.4	0.708292	0.000015	204

Country	Site	Lab code	British Museum registration numbers	$\delta^{13}C_{PDB}$ ‰	$\delta^{13}C_{PDB}$ ‰	$\delta^{18}O_{PDB}$ ‰	$\delta^{18}O_{VSMOW}$ ‰	$\delta^{18}O_{VSMOW}$ ‰	$^{87}Sr/^{86}Sr$ norm	2SE	Sr ppm
				OES	**plant***	**OES**	**OES**	**drinking water****			
Iraq	Nineveh	975	K8556 BOX 1 WAS 1.8Q (a)	-6.8	-23.0	5.6	36.7	7.6	0.708533	0.000009	407
Iraq	Nineveh	964	K8556 BOX 1 WAS 2.2Q (b)	-10.2	-26.4	3.3	34.3	3.9	0.708449	0.000009	226
Iraq	Nineveh	970	K8556 BOX 1 WAS 2.5Q (C)	-10.9	-27.1	-4.6	26.1	-8.7	0.708224	0.000011	253
Iraq	Nineveh	969	K8556 BOX 2 WAS 1.4 (a)	-8.8	-25.0	-0.8	30.1	-2.7	0.708258	0.000009	613
Iraq	Nineveh	961	K8556 BOX 2 WAS 1.7Q (C)	-10.4	-26.6	-3.3	27.6	-6.5	0.708520	0.000009	193
Iraq	Nineveh	962	K8556 BOX 2 WAS 1.8Q (c)	-10.5	-26.7	-2.0	28.8	-4.6	0.708237	0.000011	307
Iraq	Ur	990	1928.1010.705 (A)	-8.0	-24.2	0.8	31.7	-0.2	0.708034	0.000012	544

Country	Site	Lab code	British Museum registration numbers	$\delta^{13}C_{PDB}$ ‰	$\delta^{13}C_{PDB}$ ‰	$\delta^{18}O_{PDB}$ ‰	$\delta^{18}O_{VSMOW}$ ‰	$\delta^{18}O_{VSMOW}$ ‰	$^{87}Sr/^{86}Sr$ norm	2SE	Sr ppm
				OES	plant*	OES	OES	drinking water**			
Iraq	Ur	984	1928.1010.705 (B)	-8.2	-24.4	0.8	31.8	0.0	0.708018	0.000010	495
Iraq	Ur	983	1928.1010.707 (A)	-9.9	-26.1	1.9	32.9	1.6	0.708243	0.000009	408
Iraq	Ur	982	1928.1010.707(B)	-8.3	-24.5	0.6	31.6	-0.4	0.708061	0.000004	n.d.
		982	leachate 1						0.708060	0.000005	
		982	leachate 2						0.708063	0.000007	
Iraq	Ur	974	1929.1017.497 (a)	-7.6	-23.8	-0.2	30.7	-1.7	0.707992	0.000010	335
Iraq	Ur	963	1929.1017.497 (b)	-7.9	-24.1	0.0	31.0	-1.3	0.708160	0.000012	531
Iraq	Ur	973	1929.1106.7ea59727	-3.8	-20.0	8.2	39.4	11.7	0.707421	0.000011	425
Iraq	Ur	971	1930.1213.299C (a)	-6.3	-22.5	-1.5	29.4	-3.7	0.708223	0.000010	200
Iraq	Ur	967	130.1213.229C (b)	-6.3	-22.5	-1.4	29.5	-3.6	0.708221	0.000011	195

Country	Site	Lab code	British Museum registration numbers	$\delta^{13}C_{PDB}$ ‰	$\delta^{13}C_{PDB}$ ‰	$\delta^{18}O_{PDB}$ ‰	$\delta^{18}O_{VSMOW}$ ‰	$\delta^{18}O_{VSMOW}$ ‰	$^{87}Sr/^{86}Sr$ norm	2SE	Sr ppm
				OES	**plant***	**OES**	**OES**	**drinking water****			
Italy	Vulci, Isis tomb	2091	18,500,227.9 0	-10.5	-26.7	0.6	31.5	-0.4	0.709169	0.000010	62
Sudan	Northern Dongola Reach	976	2010.1001.4 79 EA85118 (BEADX4)	-1.9	-18.1	12.3	43.6	18.1	0.708494	0.000011	401
Sudan	Northern Dongola Reach	978	2010.1001.5 16 EA85155	-3.0	-19.2	10.3	41.6	15.1	0.708942	0.000010	545
Sudan	Amara West	988	F1111 Amara West	1.1	-15.1	8.1	39.2	11.5	0.709301	0.000007	514
Sudan	Amara West	992	F2288 Amara West	-0.6	-16.8	10.6	41.9	15.5	0.708087	0.000010	361
Sudan	Amara West	994	F9265 Amara West	-1.5	-17.7	11.9	43.2	17.6	0.708262	0.000010	236
Sudan	Amara West	996	F6344 Amara West	2.5	-13.7	17.6	49.0	26.5	0.707675	0.000009	595
Turkey	Tell Atchana	966	1951.0102.1 60	-8.4	-24.6	4.2	35.3	5.3	0.709101	0.000010	1251

With the exception of Anatolia and the Nubian Arabian Craton straddling the Red Sea, the bedrock of the study region is dominated by young sedimentary and igneous rocks (e.g. limestones, calcareous sandstones and basalts) of Mesozoic and Cenozoic age (Derry 1980; Asch 2005). However, many of the sites are within the Saharan or Arabian deserts and the bedrock is overlain by aeolian sediments, which in some regions are many thousands of metres thick (e.g. Rub' al Khali and the Tigris basin in Iraq (Derry 1980)). Such drift deposits will sever the link between the bedrock geology and biosphere strontium depending on the source rock of the drift. Despite different bedrock at the sites from which the archaeological OES were recovered (Table 1, main text), they produced a relatively constrained strontium isotope range (0.7074–0.7093), with the majority varying very little (i.e. 0.7080 to 0.7085), suggesting that the birds lived in environments with similar underlying rocks or unconsolidated drift such as aeolian sands (Figure 2, main text).

The mean ratios for strontium isotopes in Theban limestones and Nile sediments is reported to be 0.70777 (Burke *et al.* 1982; Touzeau *et al.* 2014). This OES range of strontium isotopes is thus consistent with limestone terrains of varying aridity or age (i.e. between the estimated lowest limestone ratio of ~0.7072 and atmospheric deposition by rain or seawater at ~0.7092 (Burke *et al.* 1982; Capo *et al.* 1998)) and is comparable with other studies of plants, animals and humans from across the study region (e.g. Buzon *et al.* 2007; Henderson *et al.* 2009; Bogaard *et al.* 2014; Hartman & Richards 2014). Such ratios may also be consistent with basalt terrains with high rainfall (e.g. >1500mm per year (Capo *et al.* 1998)), which will shift the plant ratio away from the underlying rock towards that of precipitation, thus overlapping with the limestone range, although few of the study sites have sufficient rainfall to make this a feasible interpretation (Table 1, main text). The modern farmed OES also fall within this range, but whilst all the birds were fed a diet of manufactured pellets, we have no information regarding from what or where these were produced.

One archaeological OES from Amara West, Sudan (988) has a strontium isotope ratio too high to originate from a limestone or basalt region and above the local range of 0.7073 to 0.7079 defined by Buzon *et al.* (2007), while an OES from Ur, Iraq (973) has a particularly low strontium isotope ratio (Figure S1). Both samples are significantly different to other OES found at these two sites. This suggests these were laid by birds living in different geological and hence geographical environments and is strong evidence that the strontium isotope ratios of the OES have not been entirely overlain by that of the burial environment and retain biogenic integrity. The 988 OES from Amara West may be reflecting a contribution from the rocks of the Nubian Arabian Craton, which would have ratios above 0.7092. One possible explanation for the difference between the low ratio of this OES (973) and the others found at Ur derives from work conducted on the central Anatolian plateau. Bogaard *et al.* (2014) found that plants from terraces at Çatalhöyük had strontium isotope ratios below 0.7075 whilst those on alluvial plains were higher. Similar differences may be present in the environment around Ur, but this is not proven.

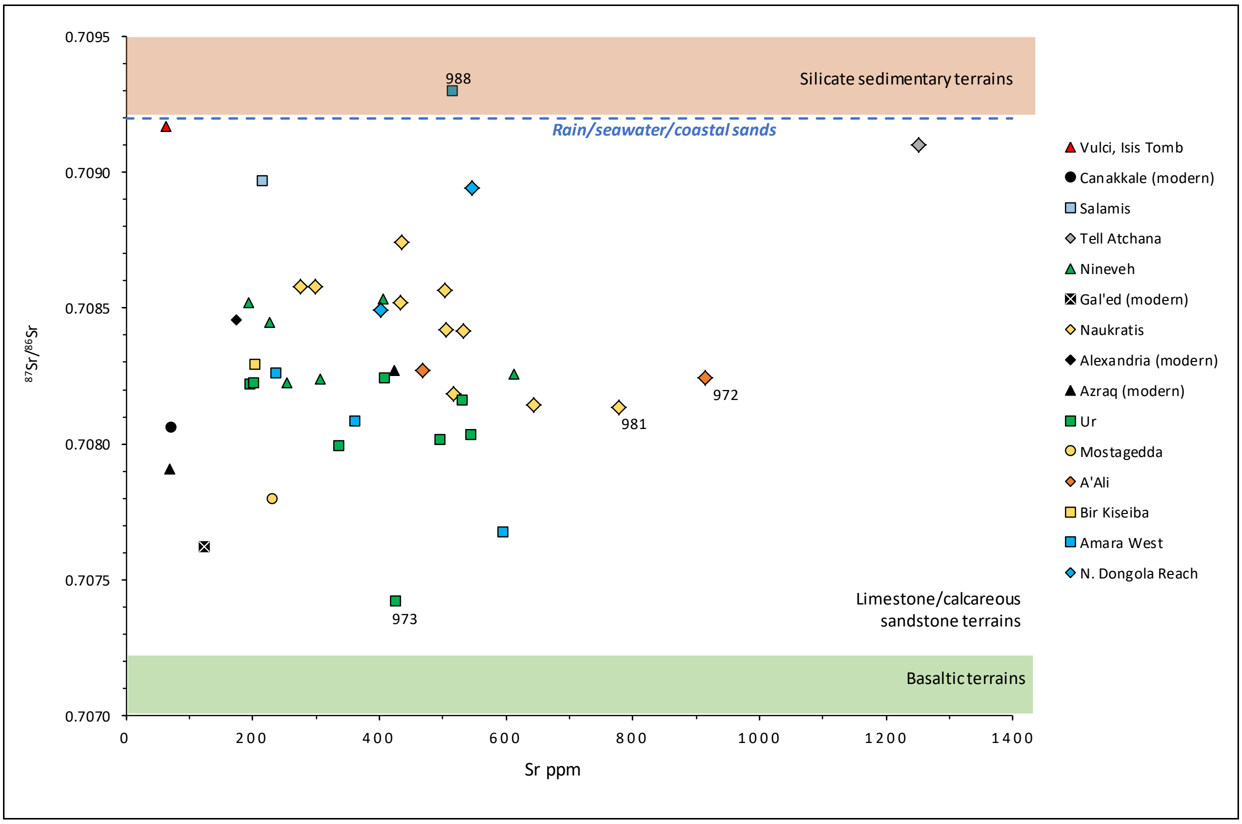

Figure S1. A plot of strontium isotope and concentrations of modern and archaeological OES. The majority of the samples have isotope ratios consistent with limestone and calcareous sandstone regions. 2sd analytical uncertainty is within the symbols.

At the two sites with the most samples, Ur and Naukratis, there is some indication that the strontium isotope ranges of OES may be reflecting an increased contribution from rain or seawater to plants ingested by the ostriches in sites closer to the coast, as most OES from Naukratis have higher strontium isotope ratios than examples from Ur (Figures S1 and S2, and Figure 2 main text). A coastal origin in a non-basaltic arid environment, e.g. in North Africa or the Middle East, would also be consistent with the three OES samples (Vulci, Salamis and Tell Atchana) which have very similar isotope characteristics (Sr, O and C) and sit just below the rain/seawater line (Figures S1 and S2). As Vulci and Salamis are assumed to have no native ostrich population, the result for Tell Atchana is the most interesting. At this site, the underlying geology is basaltic but the strontium isotope ratio of the OES analysed does not reflect this. Therefore, despite being near the coast and possibly having a local wild OES supply, the OES analysed from Tell Atchana (966) appears to have been moved to the site from a different (non-basaltic) arid coastal area.

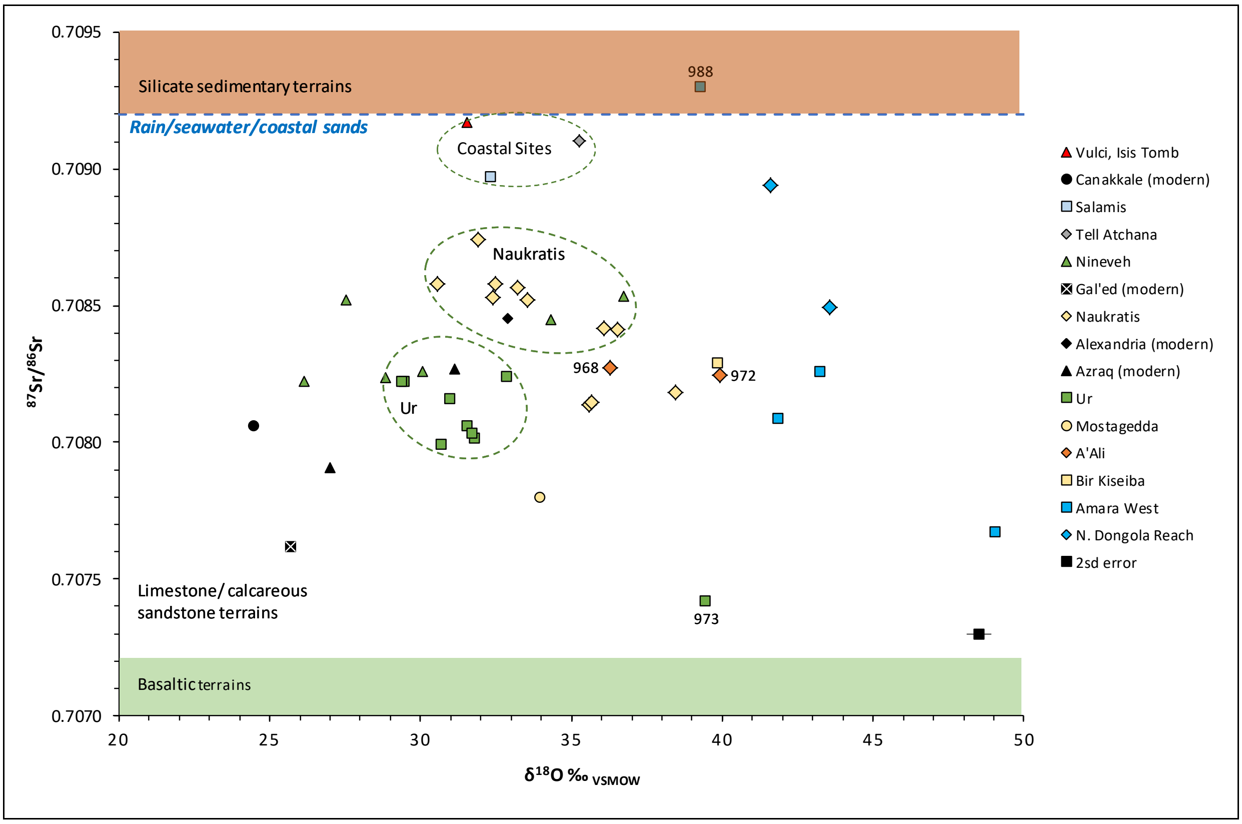

Figure S2. A plot of strontium and oxygen isotope ratios of modern and archaeological OES.

The strontium isotope ratio and concentration of modern OES was found to be variable between but not within eggs, and the concentration varies in the modern OES from approximately 70ppm to over 400ppm. There is no correlation between the amount of strontium and the isotope ratio of the OES. Some of the archaeological OES (i.e. from Tell Atchana (966), A'Ali (972) and Naukratis (981)) contain significantly more strontium (Figure S1), which may indicate post-mortem uptake by the OES. Further work, however, is needed to establish the upper limits for OES in different environments as the amount of metabolised strontium can vary with external factors such as calcium availability, coastal proximity and aridity (Freestone *et al.* 2003; Montgomery 2010), and none of the modern OES came from arid regions.

In contrast to the strontium isotope results, there is a large range in OES carbon and oxygen isotope ratios, which cluster in two main groups (Figure 3 main text). The archaeological OES are positively correlated ($r^2 = 0.57$) but these data did not correlate with strontium isotopes or concentrations. As carbon and oxygen isotope ratios increase with temperature and aridity (Hartman & Danin 2010; Miller & Fogel 2016), such a correlation is likely to be a proxy indicator of environment and increasing consumption of C_4 plants in arid and hyper-arid lower latitude environments, i.e. sites 11–15 in this study lying below 30°N. The OES oxygen isotope ratios appear to be high but for Group 1 are in line with the range (30 to 41‰) obtained by Johnson *et al*. (1998) for wild ostriches in regions of southern Africa, which are broadly comparable in temperature and rainfall to sites 1–10 located above 30°N in this study.

Johnson *et al*. (1998) found that the oxygen isotope ratios of modern wild OES, unlike farmed ones, varied widely and could not be used to establish climatic zones probably due to body water being primarily obtained from ingested plant leaf-water rather than directly from precipitation. In this study, whilst there was a general relationship of $\delta^{18}O_{OES}$ with aridity indices and latitude, there was also no direct absolute correlation between measured $\delta^{18}O_{OES}$ and that of mean annual precipitation at the site when the linear regression ($\delta^{18}O_{OES} = 31.8 + 0.65 \times \delta^{18}O_{dw;}$ Johnson *et al*. 1998: 2456) established from modern controlled ostriches was used. Anomalously high values for OES may be expected given they do not integrate annual temperatures and aridity but are mineralised and laid in a few days, usually in the warmer months of the year (Johnson *et al*. 1998).

The majority of OES samples from low latitude hyper-arid and arid sites (11–15) fall into Group 2 in Figure 3, main text) and are consistent with the eggs being laid in a similar environment to which they were found. One OES from A'Ali (968) and the sample from Mostagedda (977), however, fall into Group 1, indicating the female ostrich was consuming a 100 per cent C_3 diet and inhabiting a dry or semi-arid environment. Conversely, one OES sample from Ur (973) falls into Group 2, suggesting it was laid in an arid/hyper- arid and possibly warmer environment (see Figure 3, main text). The strontium isotope data supports this being a transported egg as it is inconsistent with the Quaternary sediments and other OES at Ur: it suggests that the female was inhabiting an arid region of limestone or regions of basalt which are found to the west in the Red Sea region in the Nubian Arabian Craton Saudia Arabia, to the east in Iran and to the south UAE (Derry 1980; Asch 2005).

The modern eggs are chiefly consistent with Group 1 but some ostriches appear to have consumed a greater proportion of C_4 plants, which may reflect a modern supply of farmed animal feed or the consumption of CAM or C_4 halophyte plants as the modern farm sites are in coastal, delta or wetland locations. C_4 or CAM consumption also appears to have been the case for one OES sample from Naukratis (993) (see Figure 3, main text). This contrasts with the other OES found at the site, and possibly the two samples from Ur, a coastal site in prehistory, which fall on the green line defining the absolute maximum carbon isotope ratio for exclusively C_3 consumers in hyper-arid environments (Kohn 2010).

Naukratis 993 also had the highest strontium isotope ratio of the eggs excavated from this site but it was not sufficiently different to separate it from the group based on strontium isotopes alone. A strong positive correlation between plant carbon isotopes and increasing aridity, for example during the dry season particularly in green plants, has been reported (Hartman & Danin 2014), and it is of note that all the OES in Group 1 fall between the cut-off for C_3 plants in hyper-arid environments (green line) and that suggested by Kohn (2010) as the lower limit of carbon isotopes for dry (i.e. annual rainfall <800mm per year) regions (blue line). There is, therefore, a gradient of decreasing rainfall from the blue to the green line in Figure 3 main text, suggesting OES closer to the blue line, such as OES from Vulci, Naukratis and Nineveh, are from higher rainfall regions than those closest to the green line, such as OES from Ur. This correlates in terms of the region's overall climate and may also be supported by the higher strontium isotope ranges, i.e. closer to rainwater, observed at Naukratis and Nineveh compared to Ur (Figure S3) although these differences are not large: variation in the fourth decimal place may be within herd or flock variability (Towers *et al*.

2017).

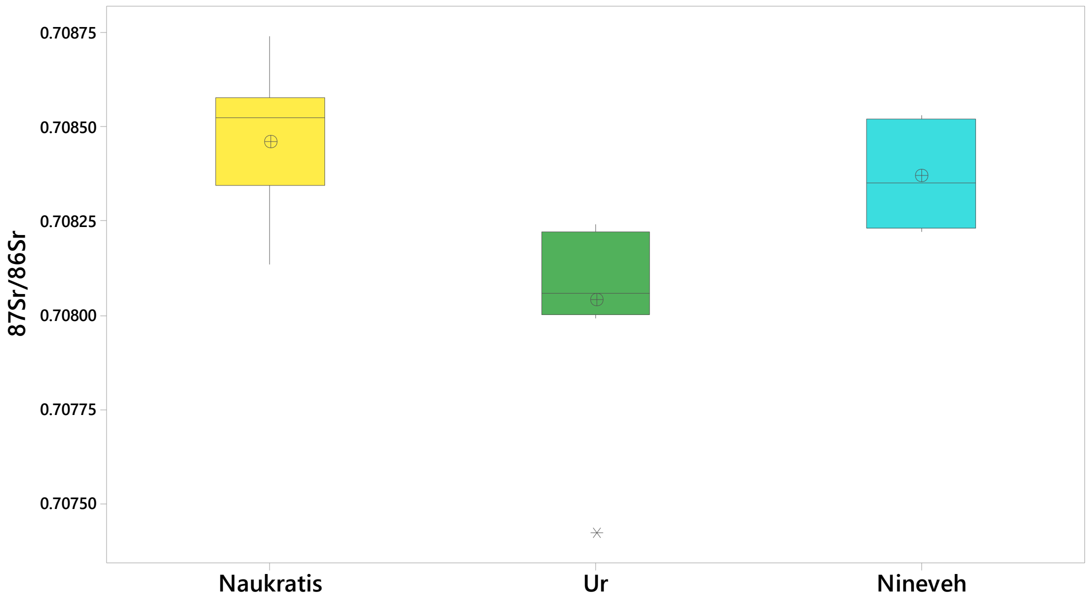

Statistics	Naukratis	Ur	Nineveh
N	10	9	6
Mean	0.70846	0.70804	0.70837
StDev	1.937E-04	2.520E-04	1.462E-04
Minimum	0.70814	0.70742	0.70822
Maximum	0.70874	0.70824	0.70853

Figure S3. Box and whisker plot and descriptive statistics for strontium isotope ratios at the three sites with six or more OES samples.

There are clear outliers or significant inter-sample variation at several of the study sites in one or more isotope systems (e.g. Figures S3–S5) although the very small sample numbers make defining the isotopic ranges for OES at the sites and further statistical exploration problematic. This implies that in regions where eggs could be sourced relatively locally, some were imported from elsewhere. This study has suggested that both isotope analysis and SEM are possible methods for identifying wild versus captive eggs and eggs that have been subject to long-distance trade across different geological zones or across different latitudes in comparison with others, found at the same site that have not moved as far. This has potentially significant implications because previously, when reconstructing the object-lives of these decorated ostrich eggs, we were able only to identify their findspot and speculate about mid-points relating to trade and decorating. Our study has highlighted source fluctuations in both the Bronze and Iron Ages; it is possible the relative values of ostrich eggs were issues affecting the trading of these luxury goods in both periods.

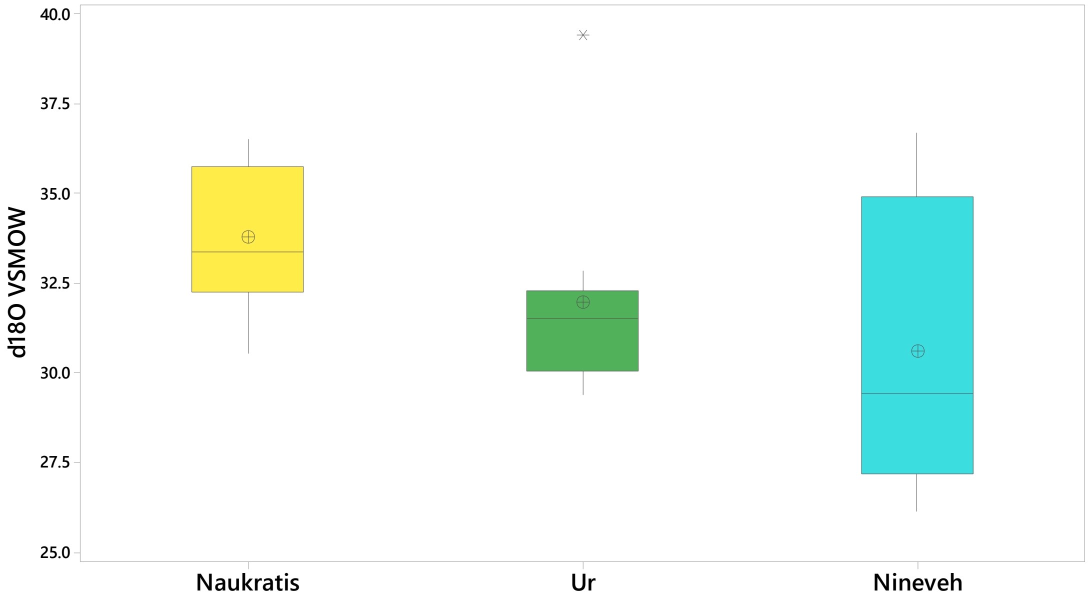

Statistics	Naukratis	Ur	Nineveh
N	10	9	6
Mean	33.799	31.980	30.603
StDev	2.0434	3.0012	4.1009
Minimum	30.550	29.388	26.138
Maximum	36.536	39.413	36.718

Figure S4. Box and whisker plot and descriptive statistics for oxygen isotope ratios at the three sites with six or more OES samples.

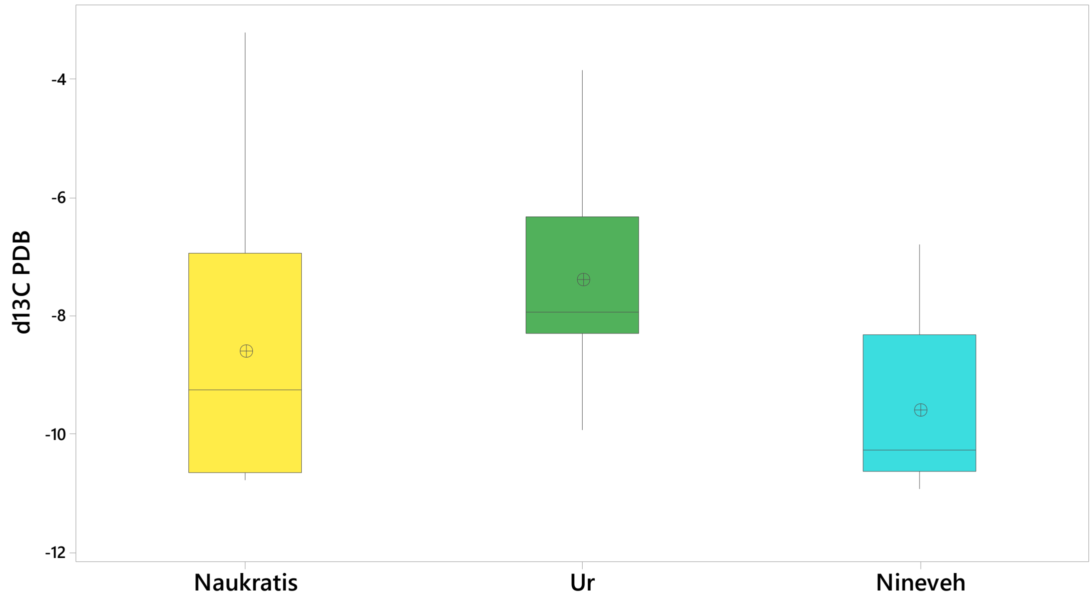

Statistics	Naukratis	Ur	Nineveh
N	10	9	6
Mean	-8.5821	-7.3791	-9.5847
StDev	2.3566	1.7176	1.5505
Minimum	-10.766	-9.9092	-10.915
Maximum	-3.2	-3.8268	-6.7796

Figure S5. Box and whisker plot and descriptive statistics for carbon isotope ratios at the three sites with six or more OES samples.

References

Asch, K. 2005. *GME 5000 geological map of Europe and adjacent areas*. Hannover: BGR.

Bogaard, A., E. Henton, J.A. Evans, K.C. Twiss, M.P. Charles, P. Vaiglova & N. Russell. 2014. Locating land use at Neolithic Catalhoyuk, Turkey: the implications of Sr-87/Sr-86 signatures in plants and sheep tooth sequences. *Archaeometry* 56: 860–77.

Burke, W.H., R.E. Denison, E.A. Hetherington, R.B. Koepnick, H.F. Nelson & J.B. Otto. 1982. Variation of sea-water ^{87}Sr/^{86}Sr throughout Phanerozoic time. *Geology* 10: 516–19.

Buzon, M.R., A. Simonetti & R.A. Creaser. 2007. Migration in the Nile Valley during the New Kingdom period: a preliminary strontium isotope study. *Journal of Archaeological Science* 34: 1391–1401. https://doi.org/10.1016/j.jas.2006.10.029

Capo, R.C., B.W. Stewart & O.A. Chadwick. 1998. Strontium isotopes as tracers of ecosystem processes: theory and methods. *Geoderma* 82: 197–225. https://doi.org/10.1016/S0016-7061(97)00102-X

CHARLIER, B.L.A., C. GINIBRE, D, MORGAN, G.M. NOWELL, D.G. PEARSON, J.P. DAVIDSON & C.J. OTTLEY. 2006. Methods for the microsampling and high-precision analysis of strontium and rubidium isotopes at single crystal scale for petrological and geochronological applications. *Chemical Geology* 232: 114–33.

CHENERY, C., V. PASHLEY, A. LAMB, H. SLOANE & J.A. EVANS. 2012. The oxygen isotope relationship between the phosphate and structural carbonate fractions of human bioapatite. *Rapid Communications in Mass Spectrometry* 26: 309–19.

COPLEN, T.B. 1988. Normalisation of oxygen and hydrogen isotope data. *Chemical Geology (Isotope Geosciences Section)* 72: 293–97.

COOPER, R.G., J.O. HORBANCZUK, R. VILLEGAS-VIZCAINO, S.K. SEBEI, A.E.F. MOHAMMED & K.M.A. MAHROSE. 2010. Wild ostrich (*Struthio camelus*) ecology and physiology. *Tropical Animal Health and Production* 42: 363–73. https://doi.org/10.1007/s11250-009-9428-2

DERRY, D.R. 1980. *A concise world atlas of geology and mineral deposits*. London: Mining Journal Books.

FREESTONE, I.C., K.A. LESLIE, M. THIRLWALL & Y. GORIN-ROSEN. 2003. Strontium isotopes in the investigation of early glass production: Byzantine and early Islamic glass from the Near East. *Archaeometry* 45: 19–32.

FRIEDLI, H., H. LOTSCHER, H. OESCHGER, U. SIEGENTHALER & B. STAUFFER. 1986. Ice core record of the $^{13}C/^{12}C$-12 ratio of atmospheric CO_2 in the past two centuries. *Nature* 324: 237–38.

HARTMAN, G. & A. DANIN. 2010. Isotopic values of plants in relation to water availability in the Eastern Mediterranean region. *Oecologia* 162: 837–52. https://doi.org/10.1007/s00442-009-1514-7

HARTMAN, G. & M. RICHARDS. 2014. Mapping and defining sources of variability in bioavailable strontium isotope ratios in the Eastern Mediterranean. *Geochimica et Cosmochimica Acta* 126: 250–64. https://doi.org/10.1016/j.gca.2013.11.015

HENDERSON, J., J.A. EVANS & Y. BARKOUDAH. 2009. The roots of provenance: glass, plants and isotopes in the Islamic Middle East. *Antiquity* 83: 414–29.

JOHNSON, B.J., M.L. FOGEL & G.H. MILLER. 1998. Stable isotopes in modern ostrich eggshell: a calibration for paleoenvironmental applications in semi-arid regions of southern Africa. *Geochimica et Cosmochimica Acta* 62: 2451–61. https://doi.org/10.1016/S0016-7037(98)00175-6

KOHN, M.J. 2010. Carbon isotope compositions of terrestrial C3 plants as indicators of (paleo)ecology and (paleo)climate. *Proceedings of the National Academy of Sciences of the USA* 107: 19691–695. https://doi.org/10.1073/pnas.1004933107
MARINO, B.D. & M.B. MCELROY. 1991. Isotopic composition of atmospheric CO_2 inferred from carbon in C4 plant cellulose. *Nature* 349: 127–31.
MILLER, G.H. & M.L. FOGEL. 2016. Calibrating delta ^{18}O in *Dromaius novaehollandiae* (emu) eggshell calcite as a paleo-aridity proxy for the Quaternary of Australia. *Geochimica et Cosmochimica Acta* 193: 1–13.
MONTGOMERY, J. 2010. Passports from the past: investigating human dispersals using strontium isotope analysis of tooth enamel. *Annals of Human Biology* 37: 325–46.
SUESS, H.E. 1958. Radioactivity of the atmosphere and hydrosphere. *Annual Review of Nuclear Science* 8: 243–56.
TOUZEAU, A., R. AMIOT, J. BLICHERT-TOFT, J.-P. FLANDROIS, F. FOUREL, V. GROSSI, F. MARTINEAU, P. RICHARDIN & C. LECUYER. 2014. Diet of ancient Egyptians inferred from stable isotope systematics. *Journal of Archaeological Science* 46: 114–24.
TOWERS, J., J. BOND, J.A. EVANS, I. MAINLAND & J. MONTGOMERY. 2017. An isotopic investigation into the origins and husbandry of Mid–Late Bronze Age cattle from Grimes Graves, Norfolk. *Journal of Archaeological Science Reports* 15: 59–72.
VON SCHIRNDING, Y., N.J. VAN DER MERWE & J.C. VOGEL. 1982. Influence of diet and age on carbon isotope ratios in ostrich eggshell. *Archaeometry* 24: 3–20.